The Korean Journal of Nuclear Medicine
Vol. 19, No. 1, May, 1985

POSITRON EMISSION TOMOGRAPHY FOR MEASURING METABOLISM *IN VIVO*

Ludwig E. Feinendegen

Institute of Medicine, Nuclear Research Center Julich GmbH and
Department of Nuclear Medicine, University Hospital Dusseldorf D-5170 Julich

Nuclear medical imaging always relates to changes at the cellular or molecular level of organization of the body. For years, such changes, summarily called metabolism, permitted radionuclides as tracers to produce information on rather gross organ structure and function. Yet, more recently, increasing emphasis is placed on metabolic reactions themselves; this development is of considerable promise to the clinician, because disease begins and nearly always expresses itself by alterations of metabolism. PET greatly helps to investigate and describe *in vivo* individual steps wihin the complex network of enzyme catalized reactions that maintain life; in fact, PET allows studies of biochemistry *in vivo*.

Method

In nuclear medicine any measurement or image relates to function which of course is linked to structure. Radionuclides when bonded to metabolites, or to equivalent compounds, permit imaging of metabolism.

Metabolism is principally measured, or imaged, through tracer accumulation, or release, in a selected region of interest as a consequence of more or less complex sequences of biochemical reactions, or, specifically, of an individual biochemical reaction.

Imaging of metabolism especially suits PET because of the advatnages[1] of observation of small volumes of tissue,[2] of quantification of tracer in situ and[3] of availability of a large number of "naturally" labelled metabolites.

Radionuclides that are natural to metabolites emit positrons, for example 11-C with a half time of about 20 minutes, 13-N with a half time of about 10 minutes, 15-0 with a half time of about 2 minutes; also useful as tracers for metabolic substrates or equivalent compounds are 18-F with a half time of 110 minutes and 75-Br with a half time of 96 minutes. Positron emitting radionuclides usually have a relatively half time; they are produced by cyclotrons and demand on line synthesis of the labelled compounds. It is for these reasons that all PET-related facilities should be close to or in a hospital.

Amongst the various positron registering instruments, most widely used and especially suitable

for dynamic sequential scintigraphy are scanners in which the detectors are placed in an orbit around the individual to be examined. Our department uses the ECAT II (of DRTEC). 66 sodium-iodide crystals are organized on to 6 bars so that each bar carries 11 crystal counters. The hexagonally placed bars are moved in synchrony around the patient in small step increments and coincidence events in crystals opposite to each other are registered, stored and used for data processing in a manner originally developed by Cormack and Hounsfield (X-ray-computerized-tomography). All signals are corrected for attenuation using a ring source of a suitable photon emitter around the patient. One to 3 million events are needed for an image of distribution of positron emitters within a transaxial slice of aobut 16mm thickness; the resolution of the system is 16 x 16mm with a medium resolution shadow shield. The instrument is geared to permit sequential images at a rate of 1-2 per minute so that time activity curves are eventually obtained from a chosen region of interest. For optimal resolution individual images are summed up and displayed on an oscilloscope screen from which regions of interest are chosen and photographs may be taken.

Quantification of substrate in tissue and speed of imaging of small volumes of tissue open the way for locally measuring the rate of substrate accumulation and release. Thus, PET has proved useful thus far for locally measuring utilization of oxygen, glucose, fatty acids, amino acids and various intermediary metabolites. Ligand binding to receptors is an interesting new development. Perfusion can be measured with suitable, labelled flow agents.

Glucose metabolism

A particular development originated from the work of Sokoloff[1] who succeeded to measure the activity of hexokinase, the enzyme that phosphorylates glucose, in the living brain of animals

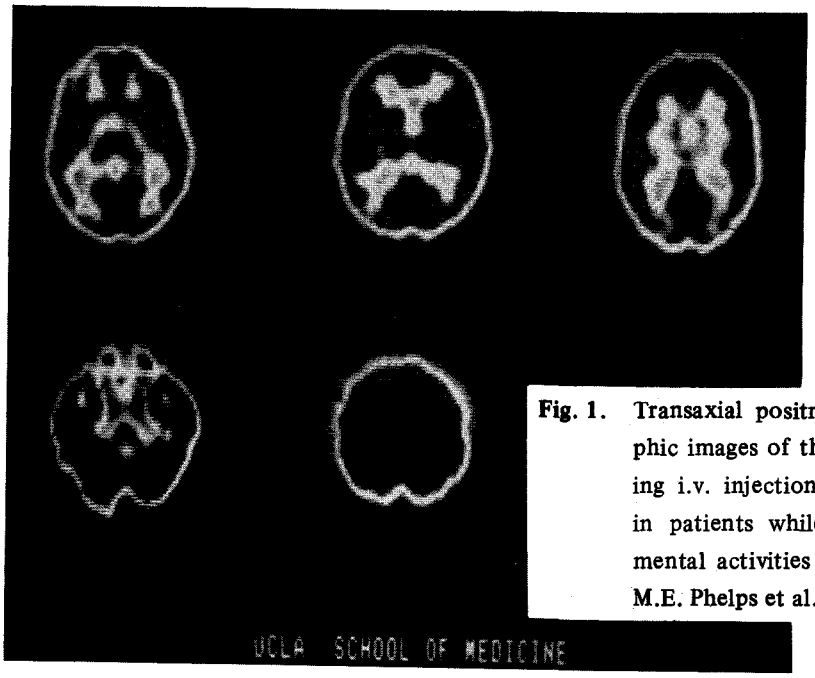

Fig. 1. Transaxial positron emission tomographic images of the human brain following i.v. injection of 18-F-deoxyglucose in patients while performing different mental activities (with permission from M.E. Phelps et al.).

by using 14-C-2-deoxyglucose and autoradiography. This tracer is trapped at the tissue site where it is phosphorylated by hexokinase; thus regional glucose utilization may be analysed. By permitting the tracer to accumulate over 30-40 minutes, the contribution from local blood flow and facilitated transport from blood into tissue to the measured rate of glucose phosphorylation is minimized. This pioneer work led to measuring the utilization of glucose in the human brain by PET and 2-18-F-deoxyglucose[2,3]. The expression of substrate quantity in terms of velocity of glucose phosphorylation and its rate constant in the human brain depends on the validation of the so-called lumped constant in the operational equation of the 2-deoxyglucose method that was developed in animal experiments[1]. This problem has not yet been fully solved but it appears that the data from the normal human brain closely reflect the activity of hexokinase. The transaxial images of normal human brains after intravenous injection of the labelled glucose analogue clearly indicate, surely in a qualitative manner, the non-homogeneous metabolic activity of the human brain[4]. The distribution of glucose utilization in the human brain is changed by various mental activities; these may be provoked for each examination, by subsequently asking the patient to see, to listen, to think, to memorize, and to act as shown by Phelps et al. in fig. 1[4]. Similar data were obtained from studies on regional cerebral blood flow by Larsen[5] and indicate the control of local blood flow by local cerebral metabolism. There are world-wide efforts now to relate such data to a variety of neurological and psychiatric disorders and one may surely expect more exciting news within the near future.

In order for the brain to function, there is not only the need for energy supply in the form of glucose but there are also interneuronal connections and effects of neuronal signal substances which bind to specific receptors.

Receptor binding in brain

An excellent example of imaging the site where signal substances are bound, is the case of dopamine and its receptor in the brain, that can be measured in man by PET and 11-C-methylspiperol, a dopamine analogue[6]. Fig. 2 shows the image of a transaxial slice cutting through the region of the caudate nucleus where the receptors of dopamine are mainly located; this data revealed moreover, that the ratio of tracer accumulation in the caudate nucleus to that in the cerebellum as a reference decreased significantly with progressing age; in females the decrease was sinificantly less than in males. – Another example is the binding of the opium analogue carfentanil, labelled with 11-C indicating the distribution of opiate receptors in the human brain, another exciting data pointing to an important development for clinical medicine[7].

Oxygen utilization

In order for the brain to fuction, oxygen is needed. The utilization of oxygen and local blood flow in the brain can be measured with 15-0[8]. Oxygen is delivered from the cyclotron to be inhaled by the patient in the form of carbon-dioxide; in the lung it is converted to 15-0 labelled water and traces the blood space. Because of the short half life of 15-0 the tissue labelling will be negligible even under steady state inhalation conditions. – Then the patient is given 15-0 as 0_2-gas

which will be linked to hemoglobin and transported into tissue where it is converted to water. Thus there will be the water of circulation and the water of metabolism. In the steady state, there is thus the potential for a dual parameter analysis, that of tissue water and of circulation water; the ratio of the two in conjunction with the 15-0_2 concentration in the circulating arterial blood is then used for calculating the regional cerebral blood flow, the oxygen extraction ratio, and the rate of cerebral oxygen metabolism.

Table 1 gives relevant data of regional cerebral blood flow, of the oxygen extraction ratio

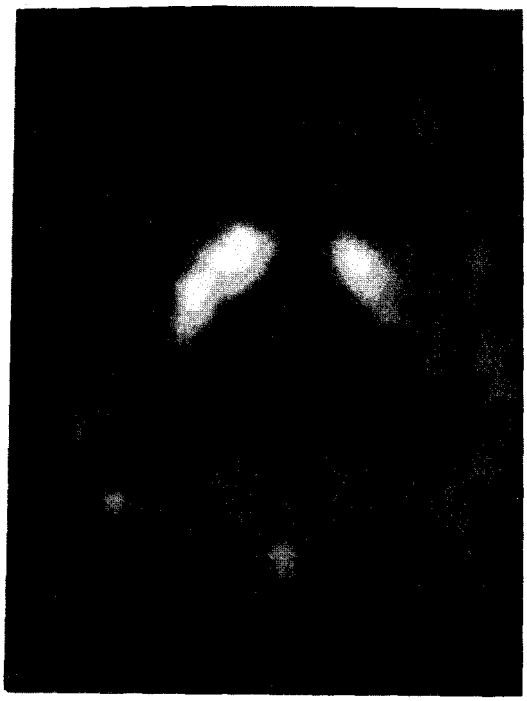

Fig. 2. Transaxial positron emisson tomographic image of the human brain following i.v. injection of 11-C-methyl-spiperol (with permission from H.N. Wagner).

Table 1. Measurement of Regional Cerebral Blood Flow, Oxygen Extraction Ratio and Regional Rate of Cerebral Oxygen Utilization Measured with 15-0-labelled CO_2 and O_2 (with permission from R.S.J. Frackowiak et al.).

	rCBF grey ml/100ml/min	rOER grey	rCMRO_2 grey mlO_2/100ml/min
NORMAL	50.8	0.53	4.69
n = 14	± 8.7	± 0.07	± 0.64
DEGENERATIVE	35.0	0.54	3.32
n = 13	± 6.9	± 0.06	± 0.43
	- 31%*	+ 2%	-29%
VASCULAR	36.5	0.53	3.29
n = 9	± 11.8	± 0.11	± 0.56
	- 28%	0	-30%

and the regional rate of cerebral oxygen utilization for gray matter of normal individuals, of patients with degenerative diseases and of patients with vascular diseases[9]. In case of vascular diease, regional cerebral blood flow is reduced whereas the oxygen extraction ratio remains normal. As a consequence the regional rate of cerebral oxygen metabolism is only moderately reduced.

Such measurements have been coupled with measurements on regional glucose utilization using 18-F-deoxyglucose[10]. In patients with stroke, the reduced regional blood flow was shown to be coupled with an increased local glucose extraction ratio; yet, the product of the two and blood sugar indicated a diminished glucose metabolism with a diminished utilization of oxygen per unit glucose uptake. – The oxygen extraction ratio was also used to monitor the evolution of ischemia to irreversible cellular damage[11]. The first study soon after onset of symptoms indicated an elevated oxygen extraction ratio; the second examination, some days after onset of symptoms in these patients, revealed the dramatic reduction of the oxygen extraction ratio and thus signaled an irreversible damage with mitochondrial breakdown.

PET in oncology

Another important area to which PET is applied, is the investigation of tumour metabolism and its response to therapy. For example, amino acid uptake was compared with local blood flow in human tumours by using 13-N-glutamate; for blood flow measurement 11-C-butanol was

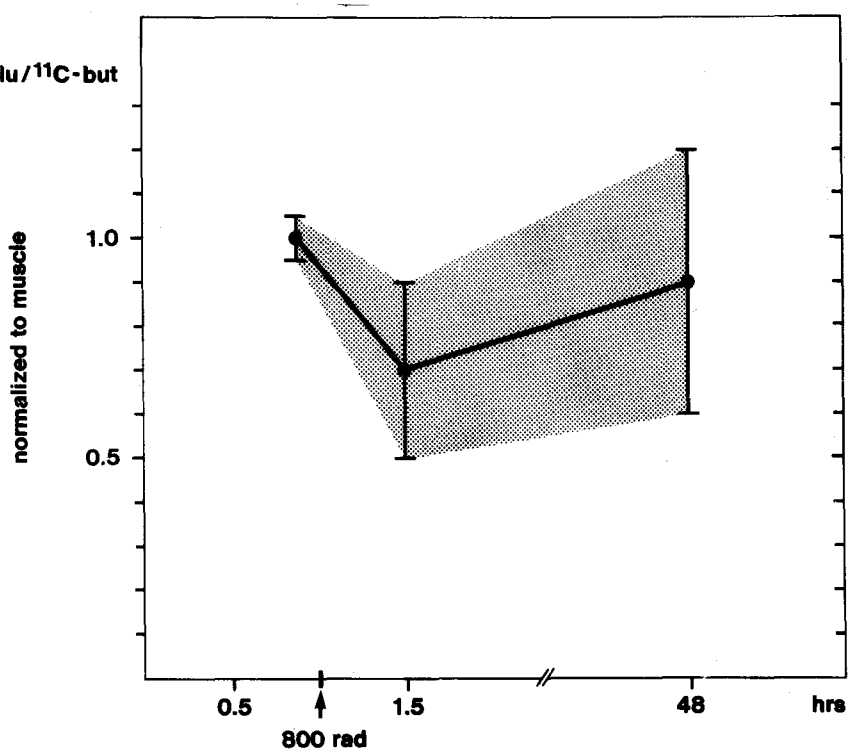

Fig. 3. Uptake of 13-N-glutamate versus local blood flow in Walker carcinoma before and after irradiation (with permission from W.H. Knapp).

chosen[12]. These data demonstrated an increased protein metabolism in a sarcoma, by normalizing glutamate uptake in the tumour to the uptake in muscle and correlating it with the corresponding perfusion data. Normally glutamate uptake was shown to be determined by local perfusion. Fig. 3 shows the change of the ratio uptake to perfusion following local radiotherapy with 800 rad; there is a drop of the ratio within 2 hours after treatment and a recovery to the starting value about 2 days later. This is a clear *in vivo* demonstration of a fast response of the tumour to radiotherapy. Such techniques may be well applied to individually tailoring therapy for a given tumour of a given individual.

Myocardial metabolism

The energy supply of the myocardium relies on fatty acids and glucose; and both can be measured effectively by PET and be related to local blood flow. It was thus demonstrated by the triple measurement of fatty acid uptake, glucose utilisation and local perfusion in fasted patients that in an ischemic myocardium the uptake of 11-C-palmitic acid is greatly reduced in concordance with the diminished blood flow, whereas glucose, in the form of 18-F-deoxyglucose, was utilized to a much greater extent than in the normal mycardium[13]. This proves that the ischemic region contained viable tissue that had changed its energy supply from fatty acids to glucose. Indeed, this triple study reveals myocardial viability and has been successfully clinically applied for example in preparation for surgery.

In many cases fatty acid analysis alone may give information on metabolic alterations in the myocardium[13-19]. Indeed, uptake and turnover of 11-C-palmitic acid were practically identical to those obtained with 123-J-omega-heptadecanoic acid that are measured by planar scintigraphy[18] as shown in fig. 4. For both tracers there is an equally rapid and a slow elimination phase; the two half times were nearly the same for both tracers in the mouse, rat and dog, with specific values for each species however[16]. The two half times relate to the turnover of different intracellular lipid pools. The correlation between the rapid and slow elimination phase alters in consequence of metabolic alterations be they on the basis of disease or induced by dietary or therapeutic intervention[13,15,18,19,20]. Especially promising is the application of labelled fatty acids for the diagnosis of cardiomyopathies[17].

Also amino acids labelled either with 11-C or 13-N have been used and they signal protein synthesis and intermediary metabolism[21]. 11-C release correlated with the production of 11-C dioxide, whereas 13-N release did not correlate with the release of 11-C-dioxide as an expression of different intracellular pathways of the two tracers.

Also acetate, pyruvate and lactate, all albelled with 11-C have been tried[13]. These compounds feed into the citric acid cycle and give information on mitochondrial function. In ischemic regions there was a decreased rate of tracer release most likely due to mitochondrial damage.

Facilitated transport of glucose

Glucose is subject to facilitated transport into tissue and cells. In the brain, this transport is

mainly governed by the blood brain barrier. Regional blood flow, glucose transport and glucose metabolism are not necessarily coupled.

Facilitated glucose transport can be separately assayed *in vivo* with 11-C-methylglucose[22,23]. In order to understand the approach to measuring specifically facilitated transport in any tissue, it is to be realized that methylglucose, like glucose and 2-deoxyglucose, is transported via the carrier system into the tissue; here, however, the pathways separate. Whereas glucose and deoxyglucose are accepted by hexokinase for phosphorylation, methylglucose was clearly shown in the brain to only enter the free glucose pool in tissue and to be transported back into the circulation[24]. There is a question whether in some tissues some methylglucose may be phosphorylated.

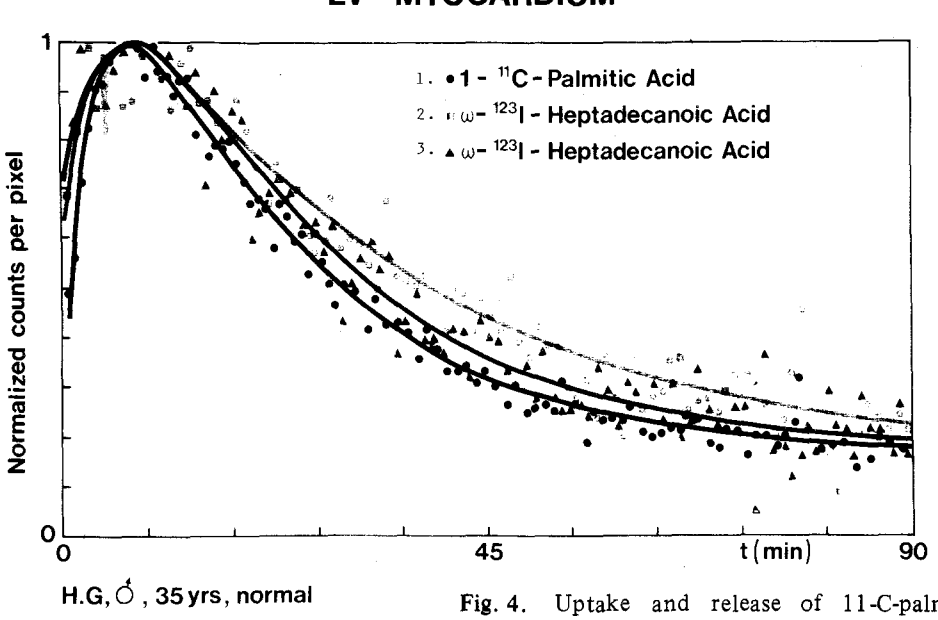

Fig. 4. Uptake and release of 11-C-palmitic acid, as measured by PET, and of omega-123-I-heptadecanoic acid, as measured by planar scintigraphy in a normal individual. Curves 1 and 3 were obtained from the patient being fully relaxed, curve 2 was obtained from the patient under mental stress (stress test) (Ref. 18).

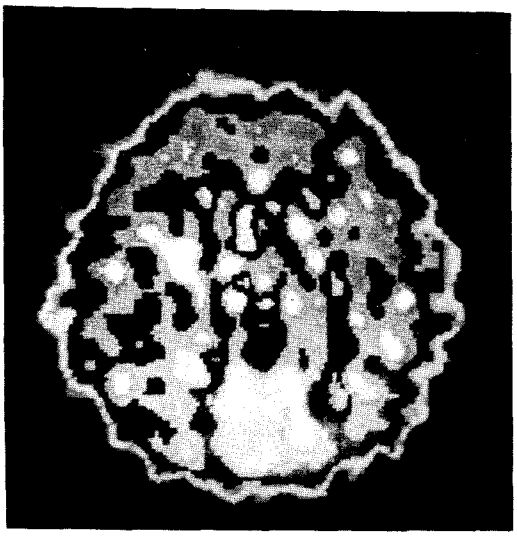

Fig. 5. Transaxial positron emission tomographic image of a normal human brain following i.v. injection of 11-C-methylglucose.

Following an intravenous pulse injection of 11-C-methylglucose, tracer concentration in brain and myocardial tissue rises to reach eventually a plateau showing the equilibrium distribution between blood and tissue; here, rate of inflow into the free glucose pool in tissue equals the rate of outflow from tissue back into circulation. A dual parameter analysis of tracer concentration in blood and tissue yields the desired rate constant of the individual biochemical reaction that is catalized by the carrier[25]. This, then, leads to the determination of the measurement of the free glucose pool in tissue, as discussed below.

Fig. 5 shows an image of 11-C-methylglucose in the normal brain, that was taken at equilibrium distribution and thus gives the tracer in the free glucose pool. This distribution is heterogenous. To arrive at the full set of the kinetic parameters describing facilitated glucose transport leading to this distribution, serial scans are obtained from a selected brain slice at 1 minute intervals following an intravenous pulse injection of 11-C-methylglucose; the tracer is measured simultaneously in the circulating blood and in tissue. The resulting two time activity curves from blood and a selected tissue region of interest in the cortex are demonstrated in Fig. 6.

These curves lend themselves to an analysis that is basically explained in Fig. 7. On the left is the model showing tracer concentration in the peripheral blood (C_B*), blood flow (f), and the tracer concentration within the tissue (C_T*); k_1* is the carrier related rate constant for inflow and k_2* the carrier related rate constant for outflow. The right side of Fig. 7 shows schematically the time activity curves of C_T* and C_B*. Following tracer injection, the curve of C_T* slowly increases to the state of equilibrium of distribution where C_T* becomes C_{Te}* with inflow, V_i*, being equal to outflow, V_e*. The rise of C_T* to C_{Te}* is expressed by the differential equation. Moreover, the derivation of the equation for [k_2*] is given. The measured [k_2*] is the ratio between increment rise in C_T* versus D_t and the difference between C_{Te}* and C_T* at any given time on the rising slope of C_T*. This [k_2*] contains also the concentration of free carrier (Hcf),

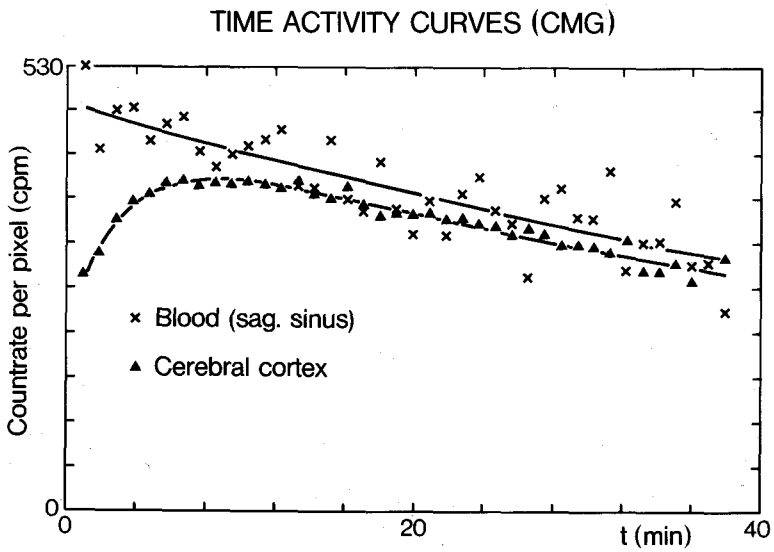

Fig. 6. Serial scintigraphy of a patient, as shown in fig. 5, permits the construction of time-activity-curves from selected regions of interest, here from the cerebral cortex and from the region sagittal sinus representing peripheral blood, per pixel (Ref. 22, 23).

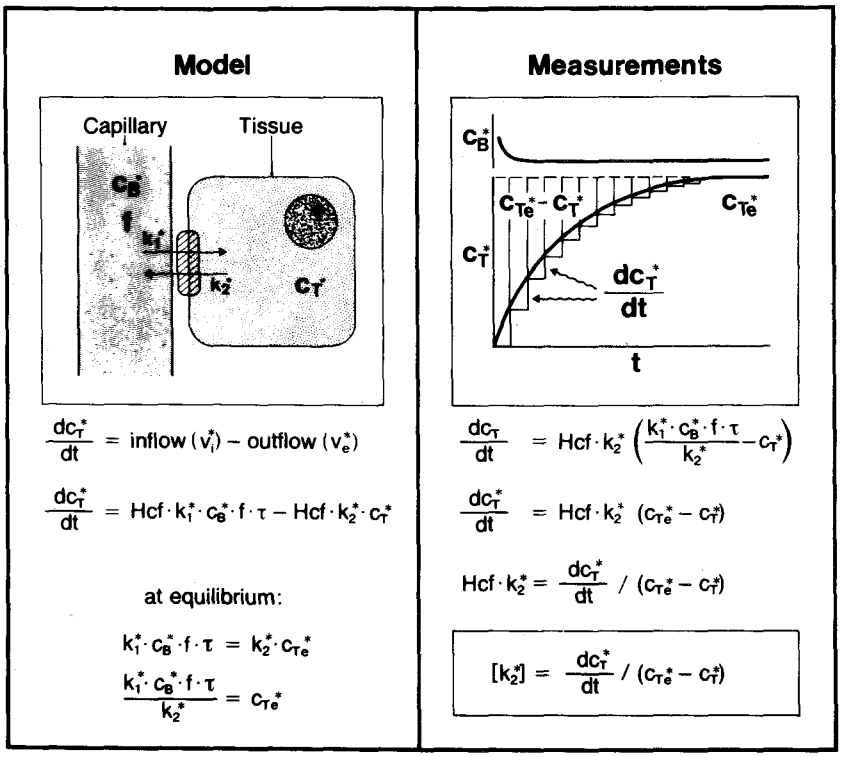

Fig. 7. Based on the model of kinetics of methylglucose transfer between blood and tissue, the dual parameters of tracer concentration in blood and tissue yield the rate constant of facilitated transport [k_2^*].

Table 2. Derivation of the Equation for Measuring the Rate of Glucose Transport from Blood into Tissue.

Calculation

Inflow of Glucose, $v_i \cdot \left(\frac{\mu M}{g \cdot min}\right)$

$$v_i = c_B \cdot f \cdot \tau \cdot [k_1]$$

since $[k_1] = [k_1^*] \cdot \xi \quad (\xi = 1.11)$

and $f \cdot \tau \cdot [k_1^*] = \frac{c_{Te}^*}{c_B^*} \cdot [k_2^*]$

$$v_i = c_B \cdot \frac{c_{Te}^*}{c_B^*} \cdot [k_2^*] \cdot \xi$$

$$\boxed{v_i = \left[\frac{\mu M}{cpm}\right]_{blood} \cdot c_{Te}^* \cdot [k_2^*] \cdot \xi}$$

Table 3. Derivation of the Equation for Measuring the Apparent Rate Constant of Glucose Transport from Blood into Tissue.

Calculation

Apparant Rate Constant of Glucose Inflow, κ_1 (min^{-1})

$$\kappa_1 = \frac{v_i}{c_B}$$

since $v_i = c_B \cdot \frac{c_{Te}^*}{c_B^*} \cdot [k_2^*] \cdot \xi$

$$\boxed{\kappa_1 = \frac{c_{Te}^*}{c_B^*} \cdot [k_2^*] \cdot \xi}$$

Table 4. Derivation of the Equation for Measuring the Michaelis-Menten-parameters for Glucose Transport, V_{max} and K_m. The Measurements are Made at two Different Blood Glucose Levles.

Calculation

Michaelis-Menten Parameters for Glucose Transport, V_{max}; K_m

$$v_i = c_B \cdot f \cdot \tau \cdot [k_1]$$

since $$[k_1] = [k_1^*] \cdot \xi \qquad (\xi = 1.11)$$

and $$f \cdot \tau \cdot [k_1^*] = \frac{c_{Te}^*}{c_B^*} \cdot [k_2^*]$$

$$v_i = c_B \cdot \frac{c_{Te}^*}{c_B^*} \cdot [k_2^*] \cdot \xi$$

$$[k_2^*] \cdot \xi = \frac{v_i}{c_B \cdot (c_{Te}^*/c_B^*)}$$

$$v_i = \frac{V_{max} \cdot S}{K_m + S}$$

since $$S = c_B \cdot \frac{c_{Te}^*}{c_B^*}$$

$$[k_2] \cdot \xi = \frac{V_{max}}{K_m + c_B \cdot (c_{Te}^*/c_B^*)}$$

$$\frac{1}{[k_2^*] \cdot \xi} = \frac{K_m}{V_{max}} + c_B \cdot \frac{c_{Te}^*}{c_B^*} \cdot \frac{1}{V_{max}}$$

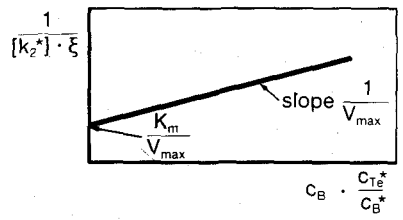

according to Michaelis-Menten equations; $[k_1^*]$, in fact, expresses $\frac{Vmax}{Km + S}$; with S being substrate concentration at the effective side of the carrier.

The three parameters, C_3^*, C_{Te}^* and $[k_2^*]$, and the glucose concentration in blood (C_B), permit the calculation not only of all kinetic parameters of the facilitated glucose transport[22,23], but also the free glucose pool in tissue[26]; an essential assumption is the application of the ratio of affinities of glucose and methylglucose to the carrier that was determined to be 1.11. The equations are shown in tables 2-5. The half maximum substrate concentration, i.e. the Michaelis-Menten constant Km, and the maximal rate of transport, Vmax, is obtained from a second measurement at a different blood glucose concentration. From 3 normal individuals, a mean value for Km of 8.2 μmol/g and for Vmax. of 2.7 μmol/g minute was found.

Table 5. Derivation of the Equation for Measuring the Free Glucose Pool in Tissue.

Calculation

Free Glucose Pool in Tissue, $c_{Te} \cdot \left(\frac{\mu M}{g}\right)$

since $$c_{Te} = \frac{v_e}{[k_2^*] \cdot \xi}$$

and $$v_e = \frac{V_{max} \cdot c_{Te}}{K_m + c_{Te}}$$

$$c_{Te} = \frac{V_{max} \cdot c_{Te}}{K_m + c_{Te}} \cdot \frac{1}{[k_2^*] \cdot \xi}$$

$$c_{Te} = \frac{V_{max}}{[k_2^*] \cdot \xi} - K_m$$

V_{max} and K_m for glucose transport can be measured with CMG.

Table 6. lists the average data from the entire cortex of 5 individuals without neurological disease. Such data are in good agreement with values obtained from animal experiments and in man[24,27,28].

This type of PET measurement appears to provide us with a most specific metabolic probe with which we can, for example, measure the effect of acute or chronic ischemia on the transport process, the effects of therapeutic intervention, for example the effect of insulin on the glucose carrier system, also in other regions of the body[29]. We can also relate such effects to those described before, for example, on the metabolic glucose utilization measured with 2-18-F-deoxy-glucose, on oxygen utilization and other metabolic reactions.

Table 6. Summary of Parameters of Glucose Transport and the Size of the Free Glucose Pool in the Entire Cortex of 5 Normal Individuals; for Calculating C_{Te}, the Average Values of V_{max} and K_m were Determined in the Cortex of Patient 1 and Two Normal Individuals, as Reported Previously[22,23]

	Patients					
	1	2	3	4	5	$x \pm \sigma$
$[k_2^*]$ [min^{-1}]	0.25	0.26	0.26	0.25	0.25	0.254 ± 0.005
c_{Te}^*/c_B^* [ml/g]	0.97	0.79	0.64	0.89	0.83	0.82 ± 0.12
c_B [μM/ml]	3.61	4.44	4.72	4.44	4.00	4.24 ± 0.44
$[k_2]$ [min^{-1}]	0.28	0.29	0.29	0.28	0.28	0.284 ± 0.005
v_i [μM/min g]	0.98	1.02	0.88	1.11	0.93	0.98 ± 0.09
κ_1 [min^{-1}]	0.27	0.23	0.19	0.24	0.23	0.23 ± 0.03
c_{Te} [μM/g]	1.49	1.16	1.16	1.49	1.49	1.35 ± 0.18

V_{max} [μM/min g] = 2.71
K_m [μM/g] = 8.18

Conclusion

The data that were here shortly reviewed point to the future of eventually describing within a defined tissue volume of interest various individual enzyme catalized reactions. This is indeed "Biochemistry *in vivo*". Such information might become of diagnostic significance for tailoring therapy especially for such groups of disorders of which we know quite little at present, for example, such as mental disorders; and there are the cardiomyopathies, degenerative diseases, malignant diseases and autoimmune diseases, where biochemical information *in vivo* might be crucial for effective treatment.

What has been achieved with PET may eventually be transferred to single photon emission

tomography and even planar scintigraphy, if and when radiopharmaceutical chemistry can produce suitable labelled compounds. Yet, it is also clear that small molecular metabolites may easily lose their biochemical specificity when labelled with a radionuclide that is foreign to the substrate and that alters stereochemical specificity and electronic configuration. For this reason, PET using radionuclides that are natural to biochemical substrates or do not alter significantly the biochemical activity of the substrate, shall remain a unique tool.

REFERENCES

1) Sokoloff L., Reivich M., Kennedy C. et al.: The (14-C) deoxyglucose method for the measurement of local cerebral glucose utilization: theory, procedure, and normal values in the conscious and anesthetized albino rat. J. Neurochem. 28, 897-916, 1977.
2) Reivich M., Kuhl D., Wolf A. et al.: The (18-F) fluoro-deoxyglucose method for the measurement of local cerebral glucose utilization in man. Circ. Res. 44, 127-137, 1979.
3) Phelps M.E., Huang S.C., Hoffman E.J., et al.: Tomographic measurement of local cerebral glucose metabolic rate in humans with (F-18) 2-fluoro-2-deoxy-D-glucose: validation of method. Ann. Neurol 6, 371-388, 1979.
4) These images were kindly supplied by Dr. M.E. Phelps, Los Angeles/USA.
5) Roland P.E., Larsen B.: Focal increase of cerebral blood flow during stereognostic testing in man. Arch. Neurol 33, 551-558, 1976.
6) Wagner H.N., Burns H.D., Dannals R.F. et al.: Imaging dopamine receptors in the human brain by positron tomography. Science 221, 1264-1266, 1983.
7) Wagner H.N., personal communcation.
8) Frackowiak R.S.J., Lenzi G.-L., Jones T. et al.: Quantitative measurement of regional cerebral blood flow and oxygen metabolism in man using 15-0 and positron emission tomography. J. Computer-Assisted Tomography 4, 727-736, 1980.
9) Frackowiak R.S.J., Pozzilli C., Legg N.J. et al.: Regional cerebral oxygen supply and utilisation in dementia: A clinical and physiological study with oxygen-15 and positron emission tomography. Brain 104, 753-778, 1981.
10) Wise R.J.S., Rhodes C.G., Gibbs J.M. et al.: Disturbance of oxidative metabolism of glucose in recent human cerebral infarcts. Ann. Neurol. 14, 627-637, 1984.
11) Wise R.J.S., Bernardi S., Frackowiak R.S.J. et al.: Serial observations on the pathophysiology of acute stroke: the transition from ischaemia to infarction as reflected in regional oxygen extraction. Brain 106, 197-222, 1983.
12) Knapp W.H., Braun A., Rohe K. et al.: Local perfusion and substrate uptake by tumors. in: Nuklearmedizin – Nuklearmedizin in Forschung und Praxis, Schmidt H.A.E., Vauramo D.E. eds., F.K. Schattauer Verlag Stuttgart-New York, 609-613, 1984.
13) Schelbert H.R.: The heart. In: Computed emission tomography, Ell P.J., Holman B.L. eds., Oxford-New York-Toronto, Oxford University Press, 91-133, 1982.
14) Feinendegen L.E., Vyska K., Freundlieb Chr. et al.: Non-invasive analysis of metabolic reactions in body tissues, the case of myocardial fatty acids. Europ. J. Nucl. Med. 6, 191-200, 1981.

15) Dudczak R., Schmoliner R., Derfler D.K. et al.: Effect of ischemia and pharmacological interventions on the myocardial elimination of I-123 heptadecanoic acid (HDA). J. Nucl. Med. 23, P34, 1982.

16) Feinendegen L.E., Shreeve W.W.: On behalf of I-123 fatty acids for myocardial metabolic imaging. J. Nucl. Med. 24, 545-546, 1983.

17) Hock A., Freundlieb Chr., Vyska K. et al.: Myocardial imaging and metabolic studies with (17-123-I)-iodo-heptadecanoic acid in patients with idiopathic congestive cardiomyopathy J. Nucl. Med. 24, 22-28, 1983.

18) Notohamiprodjo G., Schmid A., Spohr G. et al.: Comparison of myocardial metabolism of 11-C-palmitic acid (11-C-PA) and 123-I-heptadecanoic acid (123-IHA) in man. in: Nuklearmedizin-Nuklearmedizin in Forschung und Praxis, Schmidt H.A.E., Vauramo D.E. eds., F.K. Schattauer Verlag Stuttgart-New York, 233-236, 1984.

19) Notohamiprodjo G., Spohr G., Hock A. et al.: Influence of acute ethanol ingestion on myocardial fatty acid metabolism in: Radioaktive Isotope in Klinik und Forschung, Höfer R., Bergmann H. eds., Verlag H. Egermann Vienna, 755-764, 1984.

20) Beckurts T.E., Shreeve W.W., Schieren R. et al.: Kinetics of different 123-I and 14-C fatty acids in normal and diabetic rat myocardium in vivo. Nucl. Med. Comm., in press, 1985.

21) Selwyn A.P., Allan R.M., Pike V. et al.: Positive labeling of ischemic myocardium: a new approach in patients with coronary disease. Am. J. Cardiol. 47, 481, 1981.

22) Vyska K., Profant M., Schuier F., et al.: In vivo determination of kinetic parameters for glucose influx and efflux by means of 3-0-11-C-methyl-D-glucose, 18-F-3-deoxy-3-fluoro-D-glucose and dynamic positron emission tomography; theory, method and normal values. In: Current Topics in Tumor Cell Physiology and Positron-Emission Tomography, Knapp W.H., Vyska K. eds., Berlin-Heidelberg-New York-Tokyo Springer Verlag, 37-60, 1984.

23) Vyska K., Magloire J.R., Freundieb C. et al.: In vivo determination of the kinetic parameters of glucose transport in the human brain, with C-11-methyl-D-glucose (CMG) and dynamic positron emission tomography (dPET). Europ. J. Nucl. Med. in print.

24) Gjedde A., Diemer N.H.: Autoradiographic determination of regional brain glucose content. J. Cereb. Blood Flow Metab. 3, 303-310, 1983.

25) Feinendegen, L.E.: The dual parameter analysis for in vivo measuring metabolic reactions. In: Radioaktive Isotope in Klinik und Forschung 16, Höfer R., Bergmann H. eds., Verlag H. Egermann Vienna, 465-486, 1984.

26) Feinendegen L.E., Magloire J.-R., Vyska K. et al.: in preparation.

27) Sokoloff L., Smith C.B.: Basic principles underlying radioisotopic methods for assay of biochemical processes in vivo. In Lecture Notes in Biomathematics 48, Tracer Kinetics and Physiologic Modeling, Lambrecht R.M., Rescigno A. eds., Berlin-Heidelberg-New York-Tokyo Springer Verlag, 201-233, 1983.

28) Phelps M.E., Huang S.C., Hoffman E.J. et al.: Tomographic measurement of local cerebral glucose metabolic rate in humans with (F-18) 2-fluoro-2-deoxy-D-glucose: validation of method. Ann. Neurol. 6, 371-388, 1979.

29) Vyska K., Freundlieb C., Hock A. et al.: Simultaneous measurement of local perfusion rate (LPR) and glucose transport rate (LGTR) in brain and heart, with C-11-methylglucose (CMG) and dynamic positron-emission-tomography (dPET). J. Nucl. Med. 23, P13, 1982.